Article

Metal Clips Induce Folding of a Short Unstructured Peptide into an α-Helix via Turn Conformations in Water. Kinetic versus Thermodynamic Products

Rene L. Beyer, Huy N. Hoang, Trevor G. Appleton, and David P. Fairlie

J. Am. Chem. Soc., **2004**, 126 (46), 15096-15105• DOI: 10.1021/ja0453782 • Publication Date (Web): 29 October 2004

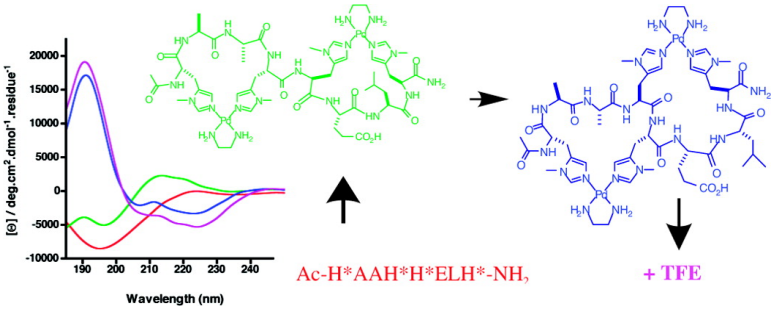

More About This Article

Additional resources and features associated with this article are available within the HTML version:

- Supporting Information
- Links to the 2 articles that cite this article, as of the time of this article download
- Access to high resolution figures
- Links to articles and content related to this article
- Copyright permission to reproduce figures and/or text from this article

View the Full Text HTML

J|A|C|S
ARTICLES
Published on Web 10/29/2004

Metal Clips Induce Folding of a Short Unstructured Peptide into an α-Helix via Turn Conformations in Water. Kinetic versus Thermodynamic Products

Renée L. Beyer,[†] Huy N. Hoang,[†] Trevor G. Appleton,[‡] and David P. Fairlie*,[†]

Contribution from the Centre for Drug Design and Development, Institute for Molecular Bioscience, and Department of Chemistry, School of Molecular and Microbial Sciences, University of Queensland, Brisbane, Qld 4072, Australia

Received July 31, 2004; E-mail: d.fairlie@imb.uq.edu.au

Abstract: Short peptides corresponding to two to four α-helical turns of proteins are not thermodynamically stable helices in water. Unstructured octapeptide Ac-His1*-Ala2-Ala3-His4*-His5*-Glu6-Leu7-His8*-NH_2 (**1**) reacts with two [Pd($^{15}NH_2(CH_2)_2{}^{15}NH_2$)($NO_3$)$_2$] in water to form a kinetically stable intermediate, [{Pden}$_2$-{(1,4)(5,8)-peptide}](**2**), in which two 19-membered metallocyclic rings stabilize two peptide turns. Slow subsequent folding to a thermodynamically more stable two-turn α-helix drives the equilibrium to [{Pden}$_2$-{(1,5)(4,8)-peptide}] (**3**), featuring two 22-membered rings. This transformation from unstructured peptide via turns to an α-helix suggests that metal clips might be useful probes for investigating peptide folding.

Introduction

Almost one-third of all amino acids in protein environments occur in α-helices,[1] typically involving two to four turns and 8−15 residues.[2] However, short peptides (<15 amino acids) corresponding to helical segments of proteins do not form thermodynamically stable α-helices in solution.[3] Nature uses a number of devices in proteins to stabilize α-helices, including histidine coordination to metal ions. Histidines in metalloproteins bind metal ions via their imidazole-N1 nitrogen (e.g. Fe in hemoglobin[4]), imidazole-N3 nitrogen (e.g. Cu in plastocyanin[5]), N1 and N3 nitrogens (e.g. Cu/Zn in superoxide dismutase[6]), or most commonly via two or more imidazole-N1 nitrogens. For example, metal ions coordinate two histidines, separated by three residues, via imidazole N1-nitrogens in hemocyanin[7] (Cu), in thermolysin (Zn),[8] and in almost 1000 human zinc finger transcription factors, where Zn^{2+} appears to stabilize an α-helix that binds to the major groove of DNA.[9] Despite the fact that such metals form a 22-membered metallocycle within helical regions in metalloproteins, relatively little is known about the capacity of metal coordination to induce or stabilize α-helicity in short peptides.[10,11] Much smaller 5- and 6-membered metallocycle chelate rings have most often been reported for short peptides bound via histidines to metals,[12] leading to a view that metal ions interact differently with proteins than with short peptides.

Of the few reports where metal ions have been claimed to stabilize α-helicity in short peptides, most have involved peptides that were already helical (e.g. Ala-rich) or conditions that favor helicity (low temperature, high ionic strength, nonaqueous solvents, unnatural constraints, etc). In those cases, metals were assumed, though not rigorously proven, to form macrocyclic chelates by coordinating to two amino acid side chains separated by three intervening residues in a sequence (e.g. i and $i + 4$ positions, as in HXXXH).[10] We have shown[11]

[†] Centre for Drug Design and Development.
[‡] Department of Chemistry.

(1) Barlow, D. J.; Thornton, J. M. *J. Mol. Biol.* **1988**, *201*, 601.
(2) Shultz, G. E.; Schirmer, R. H. *Principles of Protein Structure*, 8th ed.; Springer-Verlag: New York, 1979.
(3) (a) Zimm, B.; Bragg, J. *J. Chem. Phys.* **1959**, *31*, 526. (b) Scholtz, A.; Baldwin, R. L. *Annu. Rev. Biophys. Biomol. Struct.* **1992**, *21*, 95.
(4) Perutz, M. *Nature* **1970**, *228*, 726.
(5) Xue, Y.; Okvist, M.; Hansson, O.; Young, S. *Protein Sci.* **1998**, *7*, 2099.
(6) Messerschmidt, A.; Rossi, A.; Ladenstein, R.; Huber, R.; Bolognesi, M.; Gatti, G.; Marchesini, A.; Petruzzelli, R.; Finazzi-Agro, A. *J. Mol. Biol.* **1989**, *206*, 513.
(7) Magnus, K. A.; Hazes, B.; Ton-That, H.; Bonaventura, C.; Bonaventura, A.; Hol, W. G. *Proteins* **1994**, *19*, 302.
(8) Holland, D. R.; Hausrath, A. C.; Juers, D.; Matthews, B. W. *Protein Sci.* **1995**, *4*, 1955.
(9) (a) Greisman, H. A.; Pabo, C. O. *Science* **1997**, *275*, 657. (b) Krizek, B. A.; Amann, B. T.; Kilfoil, V. J.; Merkle, D. L.; Berg, J. M. *J. Am. Chem. Soc.* **1991**, *113*, 4518.
(10) (a) Ghadiri, M. R.; Choi, C. *J. Am. Chem. Soc.* **1990**, *112*, 1630. (b) Ruan, F.; Chen, Y.; Hopkins, P. B. *J. Am. Chem. Soc.* **1990**, *112*, 9403. (c) Ghadiri, M. R.; Fernholz, H. *J. Am. Chem. Soc.* **1990**, *112*, 9633. (d) Kohn, W. D.; Kay, C. M.; Sykes, B. D.; Hodges, R. S. *J. Am. Chem. Soc.* **1998**, *120*, 1124. (e) Kohtani, M.; Kinnear, B. S.; Jarrold, M. F. *J. Am. Chem. Soc.* **2000**, *122*, 12377. (f) Mito-Oka, Y.; Tsukiji, S.; Hiraoka, T.; Kasagi, N.; Shinkai, S.; Hamachi, I. *Tetrahedron Lett.* **2001**, *42*, 7059. (g) Hamachi, I.; Kasagi, N.; Kiyonaka, S.; Nagase, T.; Mito-oka, Y.; Shinkai, S. *Chem. Lett.* **2001**, 16.
(11) (a) Kelso, M. J.; Hoang, H.; Appleton, T. G.; Fairlie, D. P. *J. Am. Chem. Soc.* **2000**, *122*, 10488. (b) Kelso, M. J.; Hoang, H. N.; Oliver, W. N.; Sokolenko, N.; March, D. R.; Appleton, T. G.; Fairlie, D. P. *Angew. Chem. Int. Ed.* **2003**, *42*, 421. (c) Kelso, M. J.; Beyer, R. L.; Hoang, H. N.; Lakdawala, A. S.; Snyder, J. P.; Oliver, W. P.; Robertson, T. A.; Appleton, T. G.; Fairlie, D. P. *J. Am. Chem. Soc.* **2004**, *126*, 4828.
(12) (a) Hahn, M.; Wolters, D.; Sheldrick, W. S.; Hulsbergen, F.; B.; Reedijk, J. *J. Biol. Inorg. Chem.* **1999**, *4*, 412. (b) Tsiveriotis, P.; Hadjiliadis, N.; Savropoulos, G. *Inorg. Chim. Acta* **1997**, *261*, 83. (c) Milinkovic, S. U.; Parac, T. N.; Djuran, M. I.; Kostic, N. M. *J. Chem. Soc., Dalton Trans.* **1997**, 2771. (d) Sovago, I. In *Biocoordination Chemistry, Coordination Equilibria in Biologically Active Systems;* Ellis Horwood: London, 1990. (e) Tsiveriotis, P.; Hadjiliadis, N. *J. Chem. Soc., Dalton Trans.* **1999**, 459. (f) Livera, C. E.; Pettit, L. D.; Battaaille, M.; Perly, B.; Kozlowski, H.; Radomska, B. *J. Chem. Soc., Dalton Trans.* **1987**, 661. (g) Agarwal, R. P.; Perrin, D. D. *J. Chem. Soc., Dalton Trans.* **1976**, 89. (h) Ueda, J.; Ikota, N.; Hanaki, A.; Koga, K. *Inorg. Chim. Acta* **1987**, *135*, 43. (i) Kozlowski, H.; Bal, W.; Dyba, M.; Kowalik-Jankowska, T. *Coord. Chem. Rev.* **1999**, *184*, 319. (j) Parac, T. N.; Kostic, N. M. *Inorg. Chem.* **1998**, *37*, 2141.

10.1021/ja0453782 CCC: $27.50

that $[Pd(en)(NO_3)_2]$ reacts in DMF-d_7 with thermolysin fragments (Ac-H*ELTH*-NH_2, Ac-H*ELTH*AVTDY-NH_2, Ac-IDVVAH*ELTH*AVTDY-NH_2), derivatives (Ac-H*ELTH*-H*VTDH*-NH_2, Ac-H*ELTH*AVTDYH*ELTH*-NH_2, Ac-H*AAAH*H*ELTH*H*VTDH*-NH_2), or model peptides such as Ac-HAAAH-NH_2 to preferentially form one or more 22-membered chelate rings in $[\{Pd(en)\}_n(peptide)]^{2n+}$. We used histidine methylated at imidazole-N3 (H*) as a replacement for histidine (H) to direct all metal coordination via imidazole-N1, thus avoiding contamination by less preferred imidazole-N3 coordination.[11a] In all of these unstructured peptides,[11] Pd(II) formed a 22-membered macrocycle that acted as a template for inducing α-helicity in longer peptides in both C- and N-terminal directions in DMF.[11] However, there was much less α-helicity observed in water (≤40%), a feature attributed to significant competition between amide NH and water as hydrogen-bonding donors to the amide CO. Although this is probably less relevant in the hydrophobic protein environments that stabilize most α-helices, we were interested to see whether more constrained, overlapping metal chelates such as **3** (Chart 1) might increase the proportion of α-helicity in water.

In the present work we set out to investigate the helix-inducing effect of coordinating $[Pd(^{15}NH_2(CH_2)_2{}^{15}NH_2)(NO_3)_2]$ to the unstructured eight-residue peptide **1**, Ac-H*AAH*H*ELH*-NH_2 (Ac-His1*-Ala2-Ala3-His4*-His5*-Glu6-Leu7-His8*-NH_2), in water. Assuming no coordination via backbone amides or Glu carboxylate, peptide **1** has the capacity to chelate 2 equiv of $(en)Pd^{2+}$ in one of three ways, via either (H1, H4) and (H5, H8) chelation to form 19-membered rings (**2**), via (H1, H5) and (H4, H8) chelation to form 22-membered rings (**3**), or via (H1, H8) and (H4, H5) chelation to form 13- and 31-membered rings (**4**). We find that 0.2−5 equiv of $Pd(en)^{2+}$ react in water to produce initially only **2** (kinetic product), which shows evidence for peptide turn structure in water. Subsequent rearrangement produces a thermodynamic product, **3**, which exhibits well-defined α-helicity and higher per residue helicity than previously observed for metalated peptides.[11] The turns in **2** raise the possibility that turns could be important folding intermediates, trapped here only because of the stabilizing effect of metal clips. Such metal clips might be useful probes for investigating peptide folding.

Experimental Section

General. Fmoc-N3-Methyl-His-OH was obtained from Bachem AG (Switzerland). Rink amide MBHA resin and other Fmoc-L-amino acids [Fmoc-Ala-OH, Fmoc-Glu(OtBu)-OH, Fmoc-Leu-OH] were purchased from Novabiochem (Melbourne, Australia). *O*-(1*H*-6-Chlorobenzotriazole-1-yl)-1,1,3,3-tetramethyluronium hexafluorphosphate (HCTU) was obtained from Iris Biotech (Marktredwitz, Germany). All other reagents were of peptide synthesis grade and obtained from Auspep (Melbourne, Australia).

Semipreparative rp-HPLC purification of the linear peptides was performed using a Waters Delta 600 chromatography system fitted with a Waters 486 tunable absorbance detector with detection at 214 nm. Purification was performed by eluting with solvents A (0.1% TFA in water) and B (9:1 CH_3CN/H_2O, 0.1% TFA) on a Vydac C_{18} 250 × 22 mm (300 Å) steel-jacketed column at 20 mL/min. Analytical rp-HPLC analyses were performed using a Waters 600 chromatography system fitted with a Waters 996 photodiode array detector and processed using Waters Millenium software. Analytical analyses were performed using gradient elutions with solvents A and B on a Vydac C_{18} 4.6 × 250 mm (300 Å) peptide and protein column run at 1.0 mL/min.

Chart 1

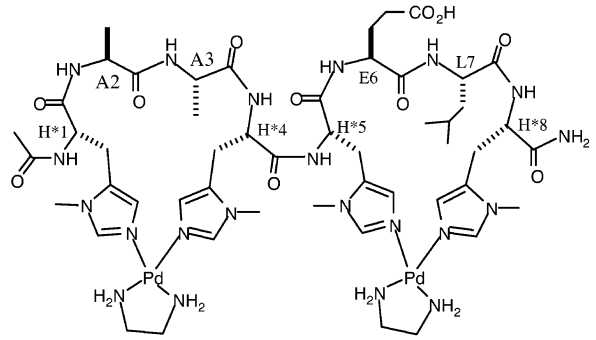

2

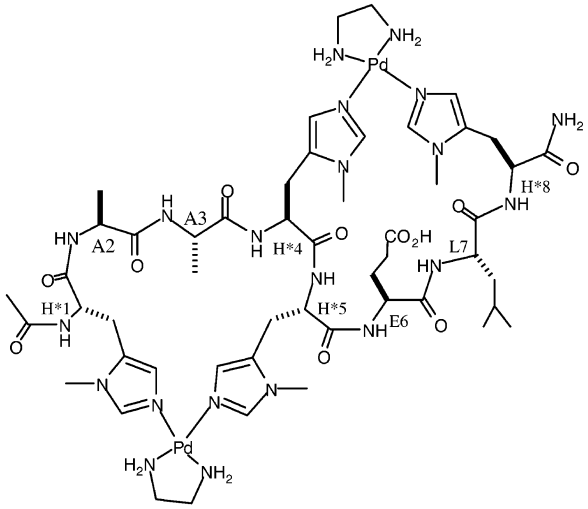

3

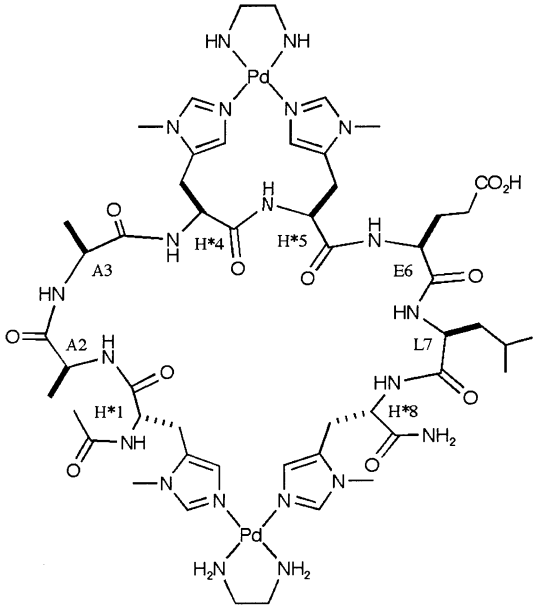

4

Synthesis and Purification of Ac-H*AAH*H*ELH*-NH_2 (1). The octapeptide Ac-His*-Ala-Ala-His*-His*-Glu-Leu-His*-NH_2 was synthesized manually by standard solid-phase methods using HCTU/DIPEA activation for Fmoc chemistry on Rink Amide MBHA resin (substitution 0.64 mmol g^{-1}, 0.25 mmol scale syntheses, 390 mg of resin). Four equivalents of Fmoc-protected amino acids, 4 equiv of HCTU, and

4.8 equiv of DIPEA were employed in each coupling (except for coupling of Fmoc-N3-Me-His-OH, where only 2 equiv of amino acid and HCTU were used). Fmoc deprotections and resin neutralization was achieved by 2 × 3 min treatments with excess 1:1 piperidine: DMF. Coupling yields were monitored by quantitative ninhydrin assay[13] and double couplings were employed for yields below 99.8%. N-Terminal acetylation was achieved by treating the fully assembled and protected peptide−resins (after removal of the N-terminal Fmoc group) with a solution containing glacial acetic acid (30 μL), DIPEA (100 μL), and 0.5 M HCTU (1 mL) in enough solution to cover the resin beds for 20 min. The peptide was cleaved from resin and protecting groups were simultaneously removed by treatment for 3 h at room temperature with a 10 mL solution containing 95% trifluoroacetic acid (TFA)/2.5% H_2O/2.5% triisopropylsilane (TIPS). TFA solutions were filtered, concentrated in vacuo, diluted with 50% A:50% B, lyophilized, and subsequently purified by semipreparative rp-HPLC using 100% A (3 min), a linear gradient of 5% to 10% B (5 min), 10% B (3 min), and finally 11% B. Yield = 28% [t_R = 11 min]. Anal. rp-HPLC (linear gradient from 0% to 100% B over 30 min): t_R = 13.5 min. MS: obsd ($M + H^+$) 1048.72, calcd 1048.54; obsd ($M + 2H^+$)/2 524.86, calcd 524.78; obsd ($M + 3H^+$)/3 350.25, calcd 350.19.

[Pd(^{15}en)(ONO$_2$)$_2$]. ^{15}en ($^{15}NH_2CH_2CH_2{}^{15}NH_2$) and [Pd(^{15}en)Cl$_2$] were prepared as described[14,15] and converted (73%) to [Pd(^{15}en)-(ONO$_2$)$_2$] as reported.[11c] Anal. Calcd for $C_2H_8N_4O_6Pd$: C, 8.27; H, 2.78; N, 19.28. Found: C, 8.25; H, 2.73; N, 18.72.

NMR Spectroscopy. Samples of metallopeptides **2** and **3** were prepared in situ by dissolving peptide **1** (3.0 mg, 2.86 μmol) in 400 μL of H_2O/D_2O (9:1). The pH was adjusted to 4.2 using 0.01 M NaOH (prepared with H_2O/D_2O, 9:1) to bring the solution volume to 553 μL, which was suitable for NMR studies. A stock solution of [Pd(^{15}en)-(ONO$_2$)$_2$] (3.5 mg, 12.0 μmol in 100 μL of H_2O/D_2O, 9:1) was prepared for titrating 2 equiv of Pd directly into the NMR tube. Titrations were monitored by 1D ^{1}H NMR spectra immediately after Pd addition. ^{1}H NMR spectra were recorded on a Bruker Avance DRX-600 spectrometer. 2D ^{1}H NMR spectra were recorded in phase-sensitive mode using time-proportional phase incrementation for quadrature detection in the t_1 dimension.[16a] 2D experiments included TOCSY (standard Bruker mlevtp or mlevph pulse programs), NOESY (standard Bruker noesytp or noesyph pulse programs), and ROESY (standard Bruker roesytp or roesyph pulse programs). TOCSY spectra were acquired over 6887 Hz with 4096 complex data points in F_2, 512 increments in F_1, and 16 scans per increment. NOESY and ROESY spectra were acquired over 6887 Hz with 4096 complex data points in F_2, 512 increments in F_1, and 48 scans per increment. TOCSY spectra were acquired with an isotropic mixing time of 80 ms. For TOCSY, NOESY, and ROESY experiments in 90% H_2O/10% D_2O, water suppression was achieved using a modified WATERGATE sequence.[16b] For 1D ^{1}H NMR spectra, the water resonance was suppressed by low power irradiation during the relaxation delay (1.5 s). Spectra were processed using XWINNMR (Bruker, Germany) software. The t_1 dimensions of all 2D spectra were zero-filled to 1024 real data points with 90° phase-shifted QSINE bell window functions applied in both dimensions followed by Fourier transformation and fifth-order polynomial baseline correction. ^{1}H NMR chemical shifts were referenced to HDO (δ 4.80 ppm) or DSS (δ 0.0 ppm) in water and $(CH_3)_2NCOD$ (δ 8.01 ppm) in DMF. $^3J_{NHC\alpha H}$ coupling constants were measured from high-resolution 1D spectra. ^{15}N NMR spectra (60.8 MHz) were obtained at 243−298 K using a DEPT pulse sequence on a Bruker Avance DRX-600 spectrometer fitted with a 5 mm broad-band tunable probe. ^{15}N chemical shifts were referenced to $^{15}NH_4^+$ (0.0 ppm) from 5 M $(^{15}NH_4)_2SO_4$ in 1 M H_2SO_4 in a coaxial capillary.

Mass Spectrometry. Positive ion electrospray mass spectra (ESMS) were recorded on a Micromass (Manchester, UK) LCT-QTOF mass spectrometer. Samples of metallopeptides **2** and **3**, prepared as for NMR analysis, were injected directly into the MS and carried to the source by a 1:1 mixture of solvents A and B (solvent A = 100% H_2O with 0.1% formic acid; solvent B = 90%CH_3CN/10% H_2O with 0.1% formic acid) at a flow rate of 100 μL min^{-1}. Mass spectra were recorded and processed with Masslynx software (version 3.5). The isotopic distribution was diagnostic for Pd (1.0% ^{102}Pd, 11.1% ^{104}Pd, 22.3% ^{105}Pd, 27.3% ^{106}Pd, 26.5% ^{108}Pd, 11.8% ^{110}Pd). To simplify peak assignment, m/z values refer to average masses calculated from average molecular weights (M) derived from the molecular formula. For complex **3**, the molecular formula ($C_{51}H_{85}N_{17}(^{15}N)_4O_{11}Pd_2$) gives an average molecular weight M = 1385.19 amu. Therefore m/z = (M/4) = 1385.19/4 = 346.30 amu. The m/z = ($M - H^+$)/3) peak was assigned a value of (1385.19 − 1.00794)/3 = 461.40 amu.

Circular Dichroism Spectra. CD measurements were made using a Jasco model J-710 spectropolarimeter calibrated with (1*S*)-(+)-10-camphorsulfonic acid. Aqueous solutions of free peptide ± 2 equiv of [Pd(^{15}en)(ONO$_2$)$_2$] were diluted into 10 mM phosphate buffer (pH 2.7 or 7.0) at 20−90 μM concentration. Temperature was controlled using a Neslab RTE-111 circulating water bath. Spectra were recorded at 277 K, with a 0.1 cm Jasco quartz cell over the wavelengths 300−185 nm at 50 nm/min (bandwidth 1.0 nm, response time 1 s, resolution step width of 0.1 nm, sensitivity 20 mdeg). Each spectrum was an average of five scans with smoothing to reduce noise. The deconvoluted spectrum for **3** in aqueous media (Figure 4) was produced by subtracting molar elipticities (185−300 nm) of product **2** (corrected to account for differences in concentration) from molar elipticities over the same wavelengths for the mixture (**2** + **3**), the resulting spectrum being adjusted for a 90 μM solution.

NMR Structural Restraints. Distance restraints for calculating the solution structure of **3** in water were derived from ROESY spectra (recorded at 298 K) using mixing times of 200−350 ms. ROE cross-peak volumes were classified as strong (upper distance constraint ≤ 2.7 Å), medium (≤3.5 Å), weak (≤5.0 Å), and very weak (≤6.0 Å), and standard pseudoatom distance corrections[17] were applied for nonstereospecifically assigned protons. Intensities were classified conservatively and only upper distance limits were included in calculations to allow the maximum number of conformers to fit experimental data. Backbone dihedral angle restraints were inferred from $^3J_{NHC\alpha H}$ coupling constants. For $^3J_{NHC\alpha H} \leq 6$ Hz, ϕ was restrained to $-65 \pm 25°$, there being single solutions to the Karplus equation over this range.[18] Seven of the eight residues in complex **3** displayed $^3J_{NHC\alpha H}$ coupling constants < 5.1 Hz, the other residue (His*8) being overlapped. No evidence for *cis*-peptide amides (i.e. no CHα-CHα i, $i + 1$ ROEs) was present in ROESY spectra, so all ω-angles were set to trans ($\omega = 180°$). Structures were calculated without hydrogen-bond restraints to prevent structure biasing.

Solution Structure Calculation. The structure of the peptide backbone in complex **3** was calculated (without Pd(en)$^{2+}$) using a dynamic simulated annealing and energy minimization protocol in X-PLOR 3.851. Initial structures with randomized ϕ and ψ angles and extended side chains were generated using an ab initio simulated annealing protocol.[19] Calculations used standard force field parameters (PARALLHDG.PRO) and topology files (TOPALLHDG.PRO) in X-PLOR with modifications to account for histidine N3-methyl groups. Structures were refined using the conjugate gradient Powell algorithm with 1000 cycles of energy minimization and a refined force-field based

(13) Sarin, V.; Kent, S. B. H. Tan, J. P.; Merrifield, R. B. *Anal. Biochem.* **1981**, *20*, 147.
(14) Appleton, T. G.; Bailey, A. J.; Bedgood, D. R., Jr.; Hall, J. R. *Inorg. Chem.* **1994**, *33*, 217.
(15) McCormack, J. B.; Jaynes, E. N.; Kaplan, R. I. *Inorg. Synth.* **1972**, *13*, 216.
(16) (a) Marion, D.; Wüthrich, K. *Biochem. Biophys. Res. Commun.* **1983**, *113*, 967. (b) Piotto, M.; Saudek, V.; Sklenar, V. *J. Biomol. NMR* **1992**, *2*, 661.
(17) Wüthrich, K.; Billeter, M.; Braun, W. *J. Mol. Biol.* **1983**, *169*, 949.
(18) Mierke, D. F.; Huber, T.; Kessler, H. *J. Comput. Aided. Mol. Design* **1994**, *8*, 29.
(19) Nilges, M.; Gronenborn, A. M.; Brünger, A. T.; Clore, G. M. *Protein Eng.* **1988**, *2*, 27.

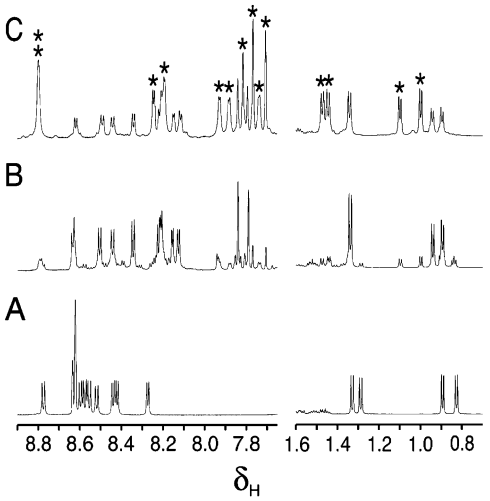

Figure 1. 1D ^{1}H NMR spectrum (amide NH, imidazole, Leu/Ala methyl regions only) of peptide **1** (3.0 mg, 2.86 μmol) in H_2O/D_2O (9:1) at pH 4.2 and 298 K: (A) alone; (B) within 60 min of adding 2 equiv of [Pd($^{15}NH_2$-$(CH_2)_2{}^{15}NH_2$)$(NO_3)_2$], showing predominantly metallopeptide **2** (ratio 9:2 for **2:3**); and (C) after 1 week, showing ~1:2 mix of **2**:**3** (*).

on CHARMm.[20] Structures were displayed in Insight II (Version 2000.1, Accelrys, San Diego, CA).

Results

1D ^{1}H NMR Spectroscopy. The reaction between **1** and [Pd-($^{15}NH_2(CH_2)_2{}^{15}NH_2$)$(NO_3)_2$] in H_2O/D_2O (9:1, pH 4.2) was monitored at 277−298 K by 1D ^{1}H NMR spectroscopy (Figure 1). Aliquots of a stock solution of [Pd($^{15}NH_2(CH_2)_2{}^{15}NH_2$)-$(NO_3)_2$] in H_2O were titrated directly into NMR tubes containing aqueous solutions of **1**. Up to 2.25 equiv of Pd produced largely one species, **2** (Figure 1B), but this transformed over several hours to a second species, **3** (Figure 1C). Addition of up to 5 equiv of Pd and subsequent heating (80 °C, 1 h) failed to change the final spectrum (Figure 1C), which indicated a ~1:2 ratio of products **2**:**3** at equilibrium.

A feature of these spectra is the increasing relative signal dispersion for **1** ≪ **2** < **3**, consistent with induction of peptide structure in both **2** and **3**. For example, simple coordination to histidines by an electrophilic palladium ion should affect the chemical shifts of imidazole atoms but cannot cause the substantial dispersion observed in the amide NH chemical shifts of **2** and **3**, which is characteristic of induction of structure. No amide NH is coordinated to palladium since all amide NH protons were clearly visible in the spectra (Figure 1). We conclude that both **2** and **3** have significant structure in water.

^{15}N NMR Spectroscopy. The reaction of **1** → **2** →**3** was also followed by ^{15}N NMR spectra (Figure 2). In water initially one species predominated (**2**, Figure 2A) after reacting **1** with [Pd($^{15}NH_2(CH_2)_2{}^{15}NH_2$)$(NO_3)_2$] in H_2O/D_2O (9:1, pH 4.2). However, after a few hours at 25 °C, two species (**2** and **3**) were clearly evident. Figure 2B shows five resonances for the 2:1 equilibrium mixture of **2** [δ_N −16.1, −16.3, −16.9 (two N)] and **3** [δ_N −16.9 (two N), −17.7, −17.9] corresponding to two products, each of which has two Pd(en)$^{2+}$ moieties bound to four different His* imidazole N1 nitrogen atoms from peptide **1**. The chemical shifts of these resonances is consistent with

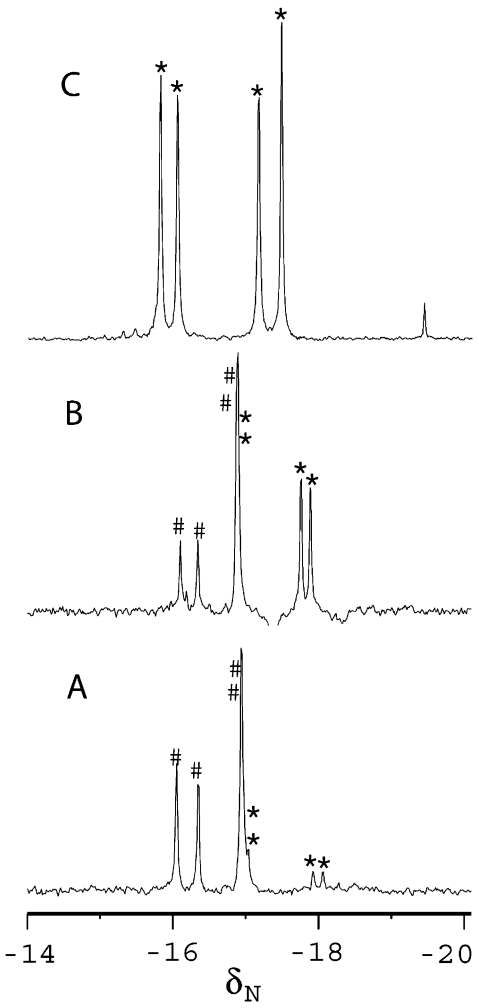

Figure 2. 60.8 MHz ^{15}N NMR spectra for reactions between peptide **1** and 2 equiv of [Pd($^{15}NH_2CH_2CH_2{}^{15}NH_2$)$(ONO_2)_2$] in H_2O/D_2O (9:1, pH 4.2, 298 K) (A) after 30 min, showing formation of mainly **2** (#), or (**B**) after 1 week, showing a ~1:2 ratio of **2** (#):**3** (*), or in DMF, (**C**) showing **3** only after 1 day. $\delta_N \sim -19$ is [Pd(en)$_2$]$^{2+}$ formed through slow subsequent disproportionation in DMF.

four inequivalent (peptide) nitrogen donor ligands, trans to four ^{15}N nitrogens of the two ethylenediamine ligands, for both **2** and **3**. None of the amide nitrogens of peptide **1** can be coordinated to Pd(II) in either metallopeptide **2** or **3** because there are nine amide NH protons detectable in ^{1}H NMR spectra for **2** and **3**.

In contrast to these observations for water, in DMF only one species (**3**, Figure 2C) was detectable at 278−298 K after addition of 2−5 equiv of [Pd($^{15}NH_2(CH_2)_2{}^{15}NH_2$)$(NO_3)_2$] to **1**. At lower temperatures (233−273 K), we were able to detect small amounts of another species (attributed to **2**), which was always in equilibrium with a greater amount of free peptide and [Pd($^{15}NH_2(CH_2)_2{}^{15}NH_2$)$(NO_3)_2$], but transformation to **3** was ~100 times faster than in water at 298 K. We conclude that species **2** is much less stable in DMF than in water and that **3** is thermodynamically more stable in DMF than in water.

Mass Spectrometry. Although the 1D and 2D NMR spectra provide compelling evidence for the stoichiometry and structural identity of complexes **2** and **3**, we sought confirmation for their (identical) molecular masses from mass spectrometry. Pd contains six naturally occurring isotopes, each Pd species

(20) Brooks, B. R.; Bruccoleri, R. E.; Olafson, B. D.; States, D. J.; Swaminathan, S.; Karplus, M. *J. Comput. Chem.* **1983**, *4*, 187.

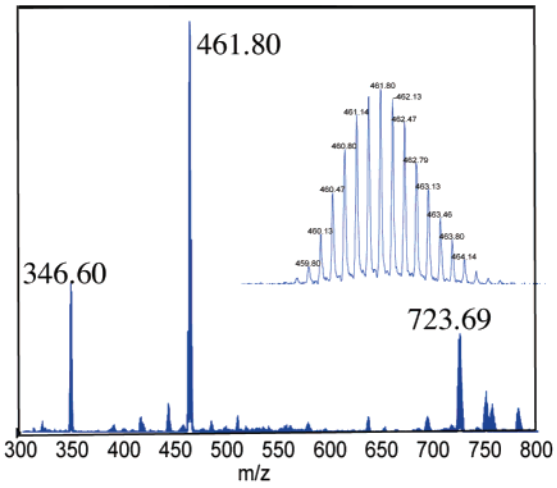

Figure 3. Electrospray mass spectra for equilibrium mixture of **2** and **3**, showing M/4 = 1386.4/4 = 346.6, (M − H^+)/3 = 1385.4/3 = 461.8, (M − H^+ + NO_3^-)/2 = 723.69. The inset shows the isotopic distribution for the middle peak. Each deconvoluted ion cluster corresponds to the theoretical cluster calculated from the molecular formula. The M − H^+ peak is attributed to deprotonation of the Glu side chain in **2** and **3**. The nitrate ion comes from the Pd reagent. Observed molecular ions and isotopic distributions prove that **1** binds to two palladiums.

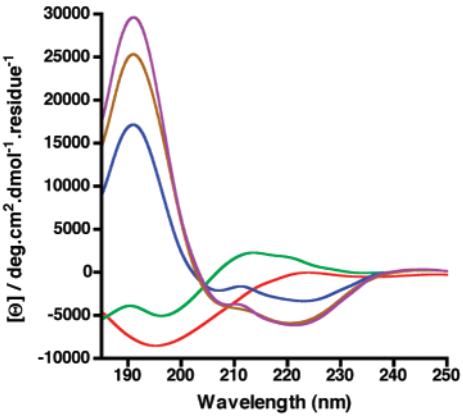

Figure 4. CD spectra for 90 μM peptide **1** (red) and after reaction with 2 equiv of [Pd(^{15}en)(ONO_2)$_2$] in aqueous 10 mM phosphate buffer (pH 2.7, 4 °C) showing **2**:**3** product ratio after 2 h (~ 20:1; green) and after several days (~ 1:1.7; blue). Deconvoluted spectrum for 100% **3** (removing contribution from **2**) is also shown (purple), and is similar to the spectrum for **3** independently isolated (100% yield) from DMF but measured in the same aqueous buffer (brown). Product ratios were determined by ^{1}H NMR spectral integration for spectra in water (pH 4.2).

exhibiting a complex cluster of isotope peaks in mass spectra. The separation between isotopes can be used to establish the charge state of the parent ion. For a 1+ ion, the isotopes are separated by 1 amu, 0.5 amu for a 2+ ion, 0.33 amu for a 3+ ion, etc. Acquiring positive ion electrospray mass spectra of peptides usually involves protonating basic species (amine, amide) to generate a detectable ion. However complexes **2** and **3** are highly charged due to the presence of 2 Pd^{2+} ions and thus need not be protonated to be observed (Figure 3).

CD Spectroscopy. Each of the three species **1**−**3** displays a quite different circular dichroism spectrum in aqueous phosphate buffer (Figure 4). Peptide **1** has no discernible structure in water, species **2** shows a turn-like ellipticity wavelength CD spectrum, while species **3** has substantial α-helical content.

α-Helical peptides (>15 residues) typically exhibit CD spectra featuring double minima (222, 208 nm) and a large positive maximum (190 nm). Percent helicity is usually calculated by the mean residue ellipticity (MRE) at 222 nm.[21] Although shorter peptides do not typically conform well to the usual relationship,[21] often leading to underestimates of α-helicity, we considered it worthwhile to calculate helicity at 222 nm for free octapeptide **1** and the metallopeptide **3** for comparison. Using the MRE at 222 nm, we calculated[21] peptide helicity for **1** (<5%) and **3** (~50%), while the positive molar elipticity for **2** at 222 nm indicates a lack of α-helicity.

Thus, while free peptide **1** has negligible helical structure in water, consistent also with a minimum ~195−200 nm typical of random structure, **3** is significantly α-helical given that the spectrum in Figure 4 represents a ~2:1 mixture of α-helical **3** and nonhelical **2**. Since 50% TFE made this equilibrium mixture <20% more helical, we wonder whether our determination of ~50% α-helicity for **3** in water might be an underestimate. The MRE ratio $[\theta]_{222}/[\theta]_{208}$ is sometimes a useful indicator of the nature of the helix, being ~0.7−1 for α-helicity but lower (~0.4−0.7) for 3_{10}-helicity.[22] We find $[\theta]_{222}/[\theta]_{208} > 1$ for the product mix **3** + **2**, despite the fact that **2** shows a positive molar elipticity at this wavelength. After deconvolution of the CD data (see Experimental Section) for the mixture of **3** + **2,** we were able to obtain a spectrum for pure **3** (Figure 4), and that spectrum had an even greater $[\theta]_{222}/[\theta]_{208}$ ratio. To check this deconvolution result, we produced **3** independently in DMF (where the equilibrium between **2** and **3** lies completely to the side of **3**), and after removing all the DMF in vacuo, we measured the CD spectrum of isolated **3** under the same aqueous conditions (Figure 4). The result was very similar to the deconvoluted spectrum.

ROESY Spectra. The ROESY spectrum of the kinetic product **2** showed some key ROE correlations between the imidazole protons of the pairs His*1-His*4 and His*5-His*8 (Figure 5). This close proximity of imidazoles in pairs His*1-His*4 and His*5-His*8 revealed that His* residues in each pair bind to only one Pd ion, as depicted in Figure 5. On the other hand, the ROESY spectrum for thermodynamic product **3** was different, showing ROE correlations between protons of His*1-His*5 and His*4-His*8 imidazole rings (Figure 5), suggesting that each of two Pd ions coordinated to His*1-His*5 and His*4-His*8, respectively. ROE correlations were also observed between amine protons on ethylenediamine and H2 protons on imidazole rings for both **2** and **3**, indicating that the Pd(en) chelate ring remained intact, leaving only two coordination sites on Pd(II) available for binding to peptide **1**.

600 MHz ROESY spectra independently characterized **2** and **3** (Supporting Information) in H_2O/D_2O (9:1). Sequence assignments[23] confirmed that **2** was the only initial product of the reaction between **1** and [Pd($^{15}NH_2(CH_2)_2{}^{15}NH_2$)($NO_3$)$_2$] in H_2O/D_2O (9:1). In ROESY spectra for **2**, connectivity was traced through only a single network of alternating intraresidue NH−Hα cross-peaks and sequential Hα−NH (*i*, *i* + 1) and HN−HN (*i*, *i* + 1) cross-peaks. No other sequential connectivities were observed, and all of the other cross-peaks in the spectrum could be assigned to just one species. In the spectra where both

(21) (a) Chen, Y.-H.; Yang, J. T.; Chau, K. H. *Biochemistry*, **1974**, *13*, 3350. (b) Lyu, P. C.; Sherman, J. C.; Chen, A.; Kallenbach, N. R. *Proc. Natl. Acad. Sci. U.S.A.* **1991**, *88*, 5317.
(22) Zhou, N. E.; Kay, C. M.; Hodges, R. S. *Biochemistry*, **1992**, *31*, 5739. (b) Garcia-Echeverria, C. *J. Am. Chem. Soc.* **1994**, *116*, 6031.
(23) Wüthrich, K. *NMR of Proteins and Nucleic Acids;* Wiley-Interscience: New York, 1986.

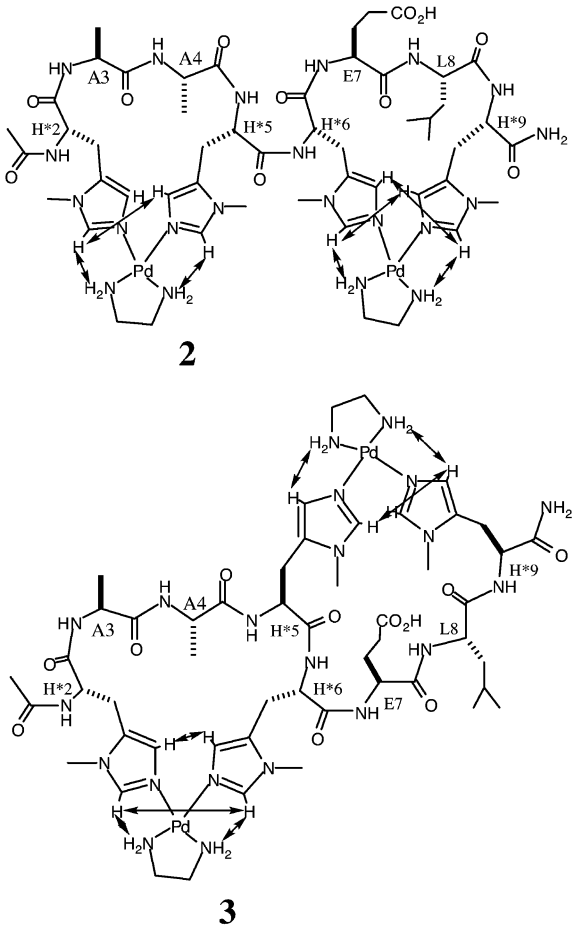

Figure 5. Identification of Pd binding modes in metallopeptides **2** and **3** by key ROE correlations.

products **2** and **3** were observed, the other sequential connectivity was due solely to product **3**, allowing assignment of cross-peaks for this species. Importantly, long range cross-peaks were observed between imidazole protons of metal-bound His* residue pairs in each complex, unambiguously revealing the Pd binding sites. None of these ROEs were present in the free peptide **1**.

$^3J_{NHC\alpha}$ Coupling Constants. The magnitude of $^3J_{NHC\alpha}$ coupling constants for each residue in peptides is dependent upon ϕ-angles[24−26] and on local conformation,[11c] three or more consecutive coupling constants <6 Hz usually being evidence of α-helical structure.[27]

Free peptide **1** has no coupling constants indicative of structure (Table 1), suggesting that it adopts only random conformations in water. Complexation with 2 equiv of Pd(II) to form **2** noticeably reduces $^3J_{NHC\alpha}$ to 3.4 Hz (Ala3) and 4.4 Hz (Leu7), while other residues showed significant, though smaller, deviations from random coil values. We conclude that metallopeptide **2** was structured, but not α-helical. It is unusual in such small peptides for backbone coupling constants to differ from the conformationally averaged value of ∼6−8 Hz,[27] so the presence of $^3J_{NHC\alpha}$ < 6 Hz for four residues, particularly

Table 1. Coupling Constants $^3J_{NHC\alpha}$ (Hz) for **1**−**3** in H_2O/D_2O (9:1) at 298 K

	$^3J_{NHC\alpha}$ (Hz)							
	His*1	Ala2	Ala3	His*4	His*5	Glu6	Leu7	His*8
1	7.6	6.0	5.8	7.7	7.4	7.1	6.9	7.8
2	6.9	5.9	3.4	7.0	6.7	5.9	4.4	7.7
3	4.3[a]	4.7[a]	3.8	5.1	4.5	4.5	4.8	*b*

[a] From dqf-COSYspectrum. [b] Could not be reliably determined.

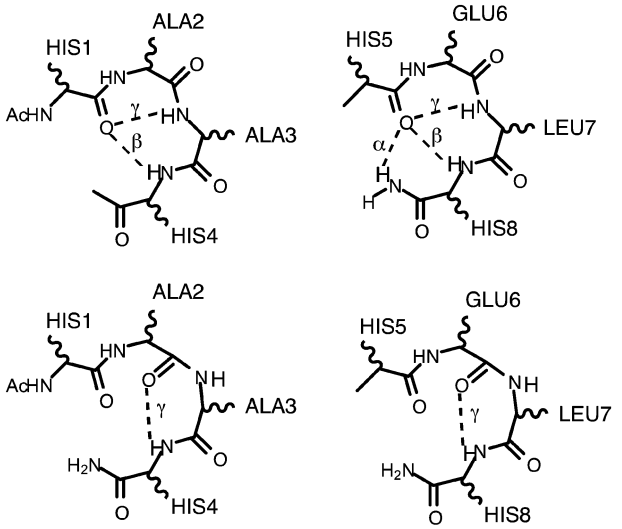

Figure 6. Some possible β- and γ-turns that may define **2**.

the significant reduction for Ala3 and Leu7, strongly suggests the presence of local structure near these residues. In contrast, the $^3J_{NHC\alpha}$ coupling constants for seven consecutive residues in metallopeptide **3** were ≤5.1 Hz, consistent with a stable α-helical structure in water.

The dihedral angles ϕ calculated for **2** from $^3J_{NHC\alpha}$ for residues Ala2, Ala3, Glu6, and Leu7 are −73°, −53°, −73°, and −61°, respectively. These angles most closely match type IV ($\phi_{i+1} = -60°$, $\phi_{i+2} = -50°$) or type III ($\phi_{i+1} = -60°$, $\phi_{i+2} = -60°$) β-turns or possibly an inverse γ-turn ($\phi_{i+1} = -79°$).[28] Interestingly, these values do not depart much from the optimal torsional angles for an α-helical backbone ($\phi_{i+1} = -59°$). These data therefore support the presence of two turns in metallopeptide **2**, centered on Ala2-Ala3 and Glu6-Leu7.

In considering which turn type might best represent the coupling constant data for **2**, Figure 6 shows some putative β- and γ-turns. If a His1 CO···HN Ala3 γ-turn is involved, it should influence $^3J_{NHC\alpha}$ for Ala2 and Ala3 (as observed), whereas a His1 CO···HN His4 β-turn should influence $^3J_{NHC\alpha}$ for Ala2 (observed) and His4 (not observed), while a γ-turn Ala2 CO···HN His4 should influence $^3J_{NHC\alpha}$ for Ala3 (observed) and His4 (not observed). Thus a γ-turn centered on Ala3 (and similarly on Leu7) would seem to be more consistent with the coupling constant data for **2**.

CH_α Chemical Shifts. Proton chemical shifts for the CH_α of peptide residues are highly sensitive to structure, in α-helices they shift upfield (>0.1 ppm) relative to random coil chemical shifts.[29] 600 MHz NOESY spectra for free peptide **1** in H_2O/

(24) Karplus, M. J. *J. Am. Chem. Soc.* **1963**, *85*, 2870.
(25) Pardi, A.; Billeter, M.; Wuthrich, K. J. *J. Mol. Biol.* **1984**, *180*, 741.
(26) Dyson, H. J.; Wright, P. E. *Annu. Rev. Biophys. Chem.* **1991**, *20*, 519.
(27) (a) Wishart, D. S.; Sykes, B. D.; Richards, F. M. *J. Mol. Biol.* **1991**, *222*, 311 (b) Wishart, D. S.; Sykes, B. D.; Richards, F. M. *Biochemistry* **1992**, *31*, 1647.
(28) (a) Nemethy, G.; Printz, M. P. *Macromolecules* **1972**, *5*, 755. (b) Venkatachalam, C. *Biopolymers* **1968**, *6*, 1425 (c) Lewis, P. N.; Momany, F. A.; Scheraga, H. A. *Biochim. Biophys. Acta* **1978**, *13*, 227 (d) Wilmot, C. M.; Thornton, J. M. *Protein Eng.* **1990**, *3*, 479.
(29) Wojcik, J.; Altmann, K.-H.; Scheraga, H. A. *Biopolymers* **1990**, *30*, 121.

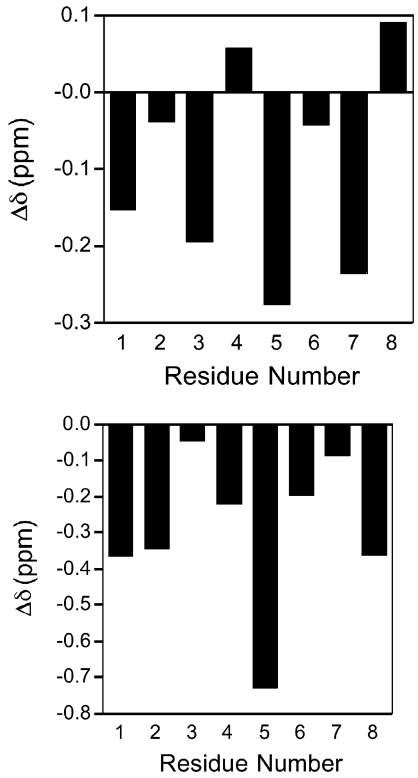

Figure 7. Upfield CHα chemical shifts in H_2O/D_2O (9:1) for **2** relative to **1** (top) and **3** relative to **1** (bottom). Negative $\Delta\delta$ values are typical of α-helicity and turns.

D_2O (9:1) showed only intraresidue and sequential cross-peaks, with no medium or long-range cross-peaks, suggesting that **1** predominantly adopts randomly extended conformations in this solvent. By comparison, for metallopeptide **2** (Figure 7) there are four of eight alternating CH_α chemical shifts (H*1, A3, H*5, and L7) that move >0.1 ppm upfield of those for the corresponding free peptide **1**. This behavior is neither typical of α-helical structure, where three or more consecutive residues normally display upfield shifts (>0.1 ppm), nor of β-strand formation, where residues normally show downfield shifts (>0.1 ppm). The data does however indicate some structure induction in **2** relative to **1**. In contrast to **1** and **2**, all CH_α chemical shifts for **3** (except for A3 and L7) are upfield (>0.1 ppm) of those for the corresponding free peptide **1** (Figure 7), supporting an α-helical structure for **3**.

Amide Proton Temperature Coefficients. The magnitude of temperature dependence of the chemical shift for an amide NH is a measure of the degree to which it is protected from solvation, most often due to hydrogen bonding.[30]For peptides, temperature coefficients ($\Delta\delta/T$) ≤ 3−4 ppb/K are consistent with involvement in an intrachain hydrogen bond such as in an α-helix or β-sheet. However, in water, all of the amide proton temperature coefficients for **2** were 7−10 ppb/K, suggesting an absence of hydrogen bonding that would be expected for helical structures. For metallopeptide **3**, amide protons expected to be involved in hydrogen bonding in an α-helical structure (H*4, H*5, E6, L7, H*8) exhibit temperature coefficients ($\Delta\delta/T$) ≤ 5 ppb/K (but only L7 had 4 ppb/K). This may reflect only weak hydrogen bonding in the helix.

ROE Distance Information. NOESY spectra were uninformative because of the molecular size of compound **3**, forcing us to resort to ROESY spectra. ROE cross-peaks in 2D-ROESY spectra of peptides usually provides evidence of structure in solution, since they are normally less dependent on factors that complicate interpretation of other spectral data.[31] Importantly, they allow conformational analysis on a per residue basis. Residues involved in α-helices are connected throughout by short $d_{\alpha N}(i,i+1)$, $d_{NN}(i,i+1)$, $d_{\alpha N}(i,i+3)$, $d_{\alpha N}(i,i+4)$, and $d_{\alpha\beta}(i,i+3)$ distances and to a lesser extent by $d_{\alpha N}(i,i+2)$ distances.[31a] ROE cross-peaks $d_{\alpha N}(i,i+1)$, $d_{NN}(i,i+1)$, $d_{\alpha N}(i,i+3)$ corresponding to these short distances occur in the ROESY spectra of complex **3** in water; however, only sequential cross-peaks were observed for complex **2**.

Solution Structure of 3. The structure for **3** in H_2O/D_2O (9:1) was calculated from 72 ROE distance restraints (36 intraresidue, 22 sequential, 14 medium range $i \rightarrow i + 3$ or $i \rightarrow i + 4$) and seven backbone ϕ-dihedral angle restraints inferred from $^3J_{NHC\alpha}$ coupling constants (Table 1). The structures were calculated in XPLOR[32] using a dynamic simulated annealing protocol in a geometric force field and were energy minimized using a modified CHARMm[20] force field. No explicit hydrogen-bond restraints were included in the structure calculations, to prevent exclusion of any non-α-helical H-bonded conformers (e.g. 3_{10}-helices).

The structure of **3**, initially calculated without $Pd(en)^{2+}$ restraints (not shown), clearly showed two i, $i + 4$ pairs of His* residues correctly oriented for coordination to Pd(II). However, in the final calculations, the N1 nitrogens of these metal-bound His* residue pairs were constrained to within 2.9 Å of each other, this separation being reported in the Cambridge crystallographic database for numerous square planar complexes with imidazole type ligands and Pd−N bond lengths of 1.90 Å. The final 20 structures chosen to represent the lowest energy conformation for **3** (Figure 8) contained no distance violations (≥0.23 Å) and no dihedral violations (≥2°), and are all very close to an idealized α-helix (rmsd = 0.27 Å) along their entire lengths, with little fraying at their N- and C-termini.

In DMF-d_7, there were much stronger ROE correlations for **3**, indicative of greater α-helicity than observed in water, and these are summarized in Figure 9. The geometry of an α-helix is characterized by short distances between protons of residues at i and $i + 3$, i and $i + 4$, and to a much less extent i and $i + 2$. The presence of medium range d_N correlations between residues with these spacings, in combination with the corresponding $d(i,i+3)$ and d_{NN} ROEs, is firm evidence for helicity in a peptide. In contrast to **3** in water, we were able to see $d_{\alpha N}(i,i+4)$, $d_{\alpha\beta}(i,i+3)$, and some $d_{\alpha N}(i,i+2)$ cross-peaks in DMF. The presence of all $d_{\alpha N}(i,i+4)$ correlations along the peptide is particularly diagnostic of α-helical rather than 3_{10}-helical or turn conformations.

Discussion

Proteins often interact with other proteins, DNA, or RNA through α-helical components, usually involving only two to four helical turns. Away from their structure-stabilizing hydro-

(30) (a) Kessler, H. *Angew. Chem., Int. Ed. Engl.* **1982**, *21*, 512 (b) Dyson, H. J.; Cross, K. J.; Houghten, R. A.; Wilson, I. A.; Lerner, R. A. *Nature* **1985**, *318*, 480.

(31) (a) Wüthrich, K.; Billeterm, M.; Braun, W. *J. Mol. Biol.* **1984**, *180*, 715. (b) Bradley, E. K.; Thomason, J. F.; Cohen, F. E.; Kosen, P. A.; Kuntz, I. D. *J. Mol. Biol.* **1990**, *215*, 607.

(32) Brünger, A. T. *X-PLOR Manual*, version 3.1; Yale University: New Haven, CT, 1992.

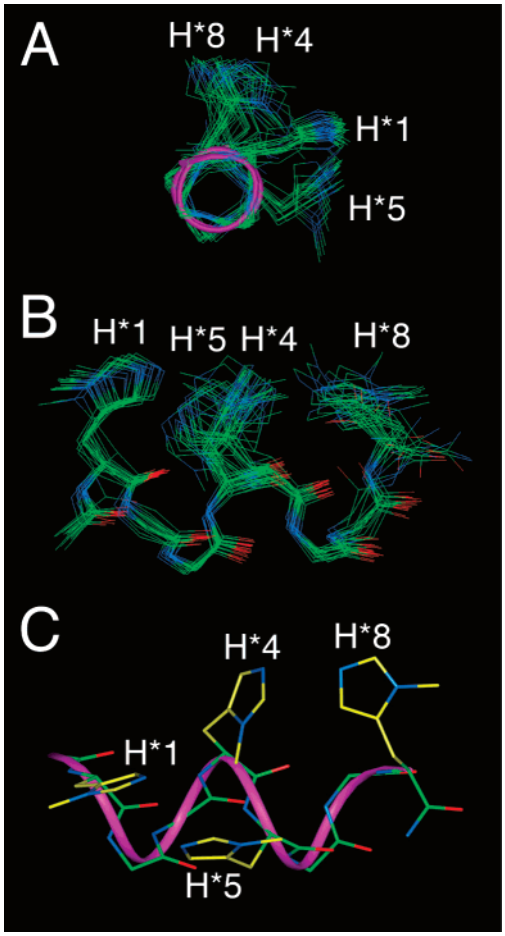

Figure 8. End (A) and side (B) views of the backbone superimposition of the 20 lowest energy calculated structures for **3** (average backbone pairwise rmsd = 0.58 Å) produced in H_2O/D_2O (9:1) at pH 4.2 from **1** (3.0 mg, 2.86 μmol) and 2 equiv of [Pd(en)$(NO_3)_2$]. Average structure (green, His* side chains yellow) compares well (C, rmsd = 0.27 Å) with the idealized α-helix (pink ribbon). Only side chains for His*, and no Pd(en) atoms, are shown for clarity.

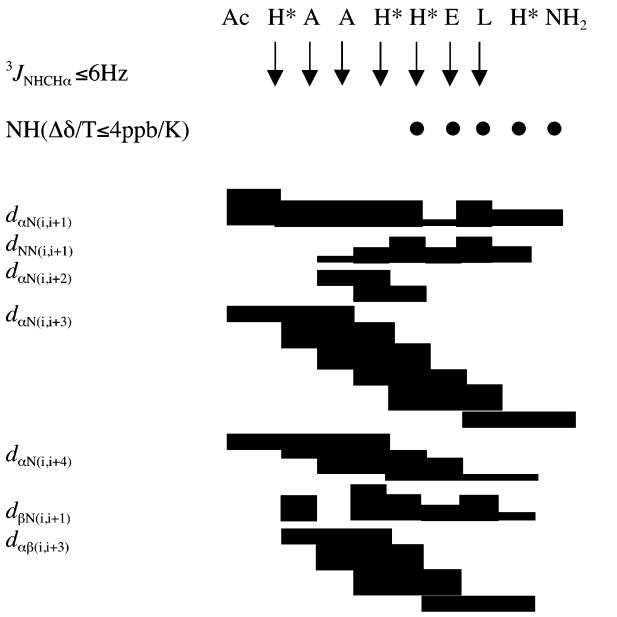

Figure 9. Summary of coupling constants $^3J_{NHCH\alpha}$ (≤6 Hz shown by ↓), amide NH temperature coefficients $\Delta\delta/T$ (≤4 ppb/K shown by ●), and ROE correlations (sequential and medium range) for metallopeptide **3** in DMF-d_7.

phobic protein environments, short α-helices are not thermodynamically stable in water.[3] Among few techniques for stabilizing short helical peptides is the use of metal ion clips that chelate to two histidines each, forming thermodynamically stable cyclic metallopeptides,[10,11] such as $[Pd(en)(H*XXXH*)]^{2+}$ (H* is histidine methylated at imidazole-N3) that represent single-turn α-helical modules. In previous work, we have shown that a pair of histidines at positions 1 and 5 (1,5) in a peptide sequence are preferred for metalation in both water and DMF over histidine pairs at (1,2), (1,6), (1,7), (1,10), (1,11), (1,15) positions.[11] The α-helicity resulting from 1,5-chelation to form a 22-membered metallocycle was pronounced in the dipolar aprotic solvent DMF, but much less in water with ∼20% α-helicity observed for [{Pd(en)}$_2${Ac-H*ELTH*H*VTDH*-NH_2}] and ∼40% for [{Pd(en)}$_3${Ac-H*AAAH*H*ELTH*H*-VTDH*-NH_2}].[11c] In an effort to increase helix induction in water, we have investigated here the potential of overlapping His-Pd-His bridges to further constrain the α-helix but have chosen to test this effect in the much smaller octapeptide Ac-H*AAH*H*ELH*-NH_2 (**1**).

There are three significant results from this new investigation. First, we show for metallopeptides in water that *i*, *i* + 3 chelation (1,4) is kinetically preferred over *i*, *i* + 4 (1,5) or *i*, *i* + 7 (1,8) bridging but that 1,5-chelation is thermodynamically more stable, though only by a factor of 2. However only 1,5-chelation results in α-helicity, which is important because *i*, *i* + 3; *i*, *i* + 4; and *i*, *i* + 7 lactam bridges are all reported[33] to increase α-helicity in longer peptides. Evidently this is not the case in the larger ring sizes of these metallopeptides.

The reaction of the octapeptide Ac-H*AAH*H*ELH*-NH_2 (**1**) with [Pd($^{15}NH_2(CH_2)_2{}^{15}NH_2$)$(NO_3)_2$] in either water or DMF leads ultimately to the metallopeptide **3**, with overlapping H*1−Pd−H*5 and H*4−Pd−H*8 bridges, as the predominant and thermodynamically most stable product. Analysis of **3** by a combination of CD spectra (Figure 4) and NMR data [CHα chemical shifts (Figure 7), $^3J_{NHCH\alpha}$ coupling constants (Table 1), ROE correlations (above)] unambiguously established that this metallopeptide has a preponderance of α-helical structure in its conformational ensemble, permitting calculation of its solution structure (Figure 8). The calculated structure was very close to an idealized α-helix. CD spectra (Figure 4) were used to calculate α-helix content for **3** in water, and the result (∼50% α-helicity) represents a somewhat higher metal-induced α-helix induction per residue than for other short peptides.[11] The shape of the CD spectrum suggests that an even higher helix content may be appropriate for this small metallopeptide than calculated from conventional formulas derived for much longer peptides. We conclude that substantial α-helicity was induced in octapeptide **1** in water through (*i*, *i* + 4) and (*i* + 3, *i* + 7) chelation to all four histidines by Pd($^{15}NH_2(CH_2)_2{}^{15}NH_2$)$^{2+}$.

A second significant result was the discovery, during formation of α-helical **3** from unstructured peptide **1**, of an interesting metallopeptide intermediate species, **2**, with side-by-side H*1−Pd−H*4 and H*5−Pd−H*8 linkages categorically established through key ROEs between histidines (Figure 5). It was surprising that **2** was kinetically preferred in water (the sole initial species) but thermodynamically unstable on the time scale

(33) Taylor, J. W. *Biopolymers* **2002**, *66*, 49.

of hours. Pd(II) usually prefers to bind specific donor atoms on the second−minutes time scale on the basis of relative thermodynamic rather than kinetic stabilities.[34]

Metallopeptide **2** transformed over hours at 25 °C ($t_{1/2}$ ∼12 h) to an equilibrium mixture of **2**:**3** in a ∼1:2 ratio. Further addition of Pd or prolonged heating failed to shift this equilibrium ratio. Thus, while **3** is thermodynamically more stable than **2**, it is only ∼2-fold more stable. Product **2** has significant structure in water as evidenced by (a) much greater chemical shift dispersion of its amide NH resonances than for free peptide **1**, similar to the dispersion seen for α-helical **3**; (b) particularly low $^3J_{NHCH\alpha}$ coupling constants for Ala3 and Leu7, corresponding to ϕ angles of −53° and −61° usually associated with β- or γ-turns but not much different to α-turns; (c) upfield shifts (>0.1 ppm) for four of eight alternating CH_α chemical shifts (H*1, A3, H*5, and L7) characteristic of turn motifs; and (d) turn-like CD spectra with positive molar elipticity maxima at 214 and 219 nm. There were however no significant ROEs to enable structure determination nor any evidence from variable temperature NMR experiments for temperature-independent amide NHs that might be expected for intramolecular H-bonds. We conclude that octapeptide **1** preferentially coordinated in water under kinetic control through (i, $i + 3$) and ($i + 4$, $i + 7$) chelation to all four histidines by $Pd(^{15}NH_2(CH_2)_2{}^{15}NH_2)^{2+}$. This product exhibits quite different CD and NMR spectra to free peptide, differences that cannot be attributed simply to the coordination of an electrophile. We further conclude that **2** consists of turn structures in water, but we were unable to identify the specific type of turn motif with certainty as there was not perfect agreement with known turn types.

It is apparent that for both **2** and **3**, two chelating $Pd(en)^{2+}$ units have imposed constraints that significantly limit conformational freedom compared with the free peptide **1**. In **3**, the two modules of $[Pd(en)(H*XXXH*)]^{2+}$ create two 22-membered rings that favor two α-turns that define an α-helix. This compound **3** is >100-fold more thermodynamically stable in DMF than **2**, which is undetectable at ambient temperatures in this solvent. In DMF formation of **3** occurred rapidly even at low temperature, indicating that the activation energy is very small in this solvent compared with water.

We interpret these results as follows. The 1,4-chelation (19-membered ring) is clearly of comparable thermodynamic stablity to 1,5-chelation (22-membered ring) in water. However, 1,5-chelation also involves the formation of multiple intramolecular hydrogen bonds that define α-helicity, and this provides additional thermodynamic driving force that makes **3** more stable than **2**. There is more competition with amide NH for amide CO from the H-bond donor solvent water than DMF, and thus H-bonds that constitute α-helicity are stronger in DMF, resulting in much higher stability and greater α-helicity for **3**. This may explain why the smaller 19-membered rings in **2** form first and are stable for hours, before slow conversion via His*4/His*5 interchange to form the 22-membered rings in **3**. We suspect that 1,4-chelation may actually be intrinsically more thermodynamically stable than 1,5-chelation, if not for the capacity of the latter to facilitate α-helix-defining intramolecular hydrogen bonds.

Third, the detection of turn structure in **2** may be important in the context of peptide folding from random coil to α-helix. There is mounting evidence for 3_{10}-helices (combinations of β-turns) being folding intermediates between random coil and α-helix in polypeptides.[35] Normally protein/peptide folding is much too fast to structurally analyze stable intermediates using the techniques herein, α-helix ↔ 3_{10}-helix interconversions occurring on subnanosecond time scales, but metal coordination may provide a means to stabilize some of these transitory folded states. The turn structure we see in **2** has been trapped out as a consequence of coordination to the metal, but we are unable to comment upon whether it is truly a folding intermediate *en route* to peptide α-helix in the absence of the metal. In any case, what we have succeeded in doing is to slow the rate of folding of an α-helix to a time scale of hours (**2**→**3**), and this may be a valuable technique for investigating peptide folding.

The sequences HXXH and HXXXH are very common signatures in proteins (occurring many thousands of times in the Swiss protein sequence database) and represent potential metal-binding domains. The present study was therefore important in identifying their relative capacities for both binding to a metal ion and inducing formation of α-helical peptide structure. The finding that both motifs have reasonably comparable affinities and stabilities in metallopeptides, but that only HXXXH favors α-helicity, is interesting and adds further weight to our recent studies suggesting that the 22-membered metallocycle uniquely templates helix induction. By contrast the HXXH signature, exemplified in this study by HAAH and HELH, binds to the metal ion to form 19-membered metallocycles that have higher kinetic stability than the 22-membered ring formed from HXXXH.

This work points to the possibility that polypeptides might transiently accommodate first row transition metals at multiple sites in a peptide sequence, forming kinetically labile (turn) complexes that might assist folding by lowering the activation energy needed to ultimately form thermodynamically stable helical structures. Like the kinetically labile Pd^{2+}, first row transition metals may then shuffle along to their final resting place or come off altogether after facilitating formation of a thermodynamically stable helix and protein structure. The potential of metal ions as folding tools clearly needs to be investigated in greater detail, recognizing that kinetic products may not be easily detectable for rapidly exchanging metal ions.

In summary, this work demonstrates that metal ions can have powerful influences on peptide folding. Here we have induced folding of an unstructured peptide into an α-helix, and by changing solvent and metal-coordination sites, we have regulated both the rate and extent of α-helix folding. This control illustrates promising uses of small metallopeptides for studying peptide folding, modeling protein folding, and possibly using metal ions as folding tools in ways that Nature may already use. It remains to be seen whether modified helix-inducing metal complexes can be developed into reversible clips on peptides and proteins as general protein-folding devices.

Abbreviations. DIPEA, diisopropylethylamine; DMF, *N*,*N*-dimethylformamide; ESI-MS, electrospray ionization mass spectrometry; MBHA, methylbenzhydrylamine; rp-HPLC, re-

(34) Appleton, T. G. *Coord. Chem. Rev.* **1997**, *166*, 313.

(35) (a) Toniolo, C.; Benedetti, E. *Trends Biochem. Sci.* **1991**, *16*, 350. (b) Dehner, A.; Planker, E.; Gemmecker, G.; Broxterman, Q. B.; Bisson, W.; Formaggio, F.; Crisma, M.; Toniolo, C.; and Kessler, H. *J. Am. Chem. Soc.* **2001**, *123*, 6678. (c) Cordes, M. H.; Walsh, N. P.; McKnight, C. J.; Sauer, R. T. *J. Mol. Biol.* **2003**, *326*, 899. (d) Pengo, P.; Pasquato, L.; Moro, S.; Brigo, A.; Fogolari, F.; Broxterman, Q. B.; Kaptein, B.; and Scrimin, P. *Angew. Chem. Int. Ed.* **2003**, *42*, 3388.

versed-phase high-performance liquid chromatography; TFA, trifluoroacetic acid, HCTU, *O*-(1*H*-6-chlorobenzotriazole-1-yl)-1,1,3,3-tetramethyluronium hexafluorphosphate.

Acknowledgment. We thank the Australian Research Council for partly supporting this research and for an Australian Professorial Fellowship (D.P.F.).

Supporting Information Available: Figures S1−S5 and Tables S1and S2 provide TOCSY, NOESY and ROESY data for **1**−**3**. This material is available free of charge via the Internet at http://pubs.acs.org.

JA0453782